13th ewtec 2019 Proceedings of the 13th European Wave and Tidal Energy Conference 1-6 Sept 2019, Naples, Italy

# Modelling the wake of a tidal turbine with upstream turbulence: LBM-LES versus Navier-Stokes LES

Mikael Grondeau, Jean-Charles Poirier, Sylvain Guillou,
Yann Méar, Philippe Mercier, Emmanuel Poizot

***Abstract*—Tidal turbines are entering an industrial phase and farms will soon be installed. In order to optimize the power output of tidal farms, a good understanding of the interactions between the ambient turbulence and a single turbine is crucial. Computational Fluid Dynamics, and more precisely Large Eddy Simulation, is one way of acquiring such knowledge. This study proposed a comparison between a Lattice Boltzamnn Method LES approach and a Navier-Stokes LES approach to model the wake of a tidal turbine. Numerical results are compared with experimental results and a relatively good concordance is observed. Differences inherent to the approaches are then pointed out.**

***Index Terms*—Tidal turbine, turbulence, numerical modelling, Large Eddy Simulation, Lattice Boltzmann Method, Navier-Stokes.**

## I. Introduction

TIDAL turbines are Marine Renewable Energy (MRE) devices that extract the kinetic energy from tidal currents. Most of tidal turbines only work in areas where tidal currents are over $2.0 m.s^{-1}$. All those sites are characterized by high turbulence rates. For example, turbulence rate at EMEC site, Fall of Warness, is around 10 % [1]. Turbulence acts on the machine in several ways [2]. It can affects the power coefficient [3] and the wake [4]. Like wind turbines, tidal turbines will be set up in farms in order to maximize energy extraction and reduce costs. A good knowledge of the wake of a single tidal turbine in a turbulent flow is therefore essential to optimize the layout of a farm.

In situ field measurements and experimental data are expensive to acquire. Computational Fluid Dynamics (CFD) is an interesting way of predicting turbines behaviour at moderate cost. Indeed, LES studies have already been used to predict the behaviour of tidal turbines. Ouro *et al.* (2017) [5] have used an IBM-LES model to successfully compute the wake behind a vertical axis tidal turbine. Ahmed *et al.* (2017) [6] have also used an LES approach to compute blades loadings of a horizontal axis tidal turbine. The study presented here uses a Lattice Boltzmann Method (LBM) LES and a Navier-Stokes (NS) LES model to compute the wake of a tidal turbine. The LBM is an unsteady CFD method. It is explicit and low dissipative. It is thus quite efficient to compute large volumes needed for wake studies. However, it is rarely used for MRE studies which is why a NS approach is also performed. The NS study is carried out with robust models from a commercial software. It provides state-of-the-art NS results and makes it possible to be more critical regarding the LBM capacity for blade resolved MRE studies.

First section presents the reference experiment, numerical models and meshes used for the LBM and NS studies. The LBM being relatively new in MRE field, some details about the method are presented. The second section presents results of both approaches. The last section gives the conclusion and prospects of this work.

## II. Materials and methods

### A. Reference experiment

The reference experiment is presented in Mycek *et al.* (2014) [4]. It was carried out at Ifremer flume tank in Boulogne-sur-Mer (France) and gives the performance and wake of a three-bladed horizontal axis tidal turbine with turbulent inflow conditions. The tidal turbine is visible in Fig. 1.

The tidal turbine was tested with two turbulent inflow conditions: $I = 3$ % and $I = 15$ %. $I$ is the turbulence rate defined in Equation (1). The turbine was also tested with several sets of parameters. The sets chosen for the simulations are listed in Table I.

$$I = 100\frac{< u' >}{< U >}, \tag{1}$$

$$< u' >= \sqrt{\frac{1}{3}(< u_x'^2 > + < u_y'^2 > + < u_z'^2 >)}, \tag{2}$$

Paper ID: 1618. Paper track: THM. This work was supported by ANRT CIFRE contract number 2015/1194. Computational means were founded by Manche County Concil and provided by CRIANN computational center.

M. Grondeau is with the University of Caen, LUSAC, 60 rue Max-Pol Foucher, CS20082, Cherbourg, France (e-mail: mikael.grondeau@unicaen.fr).

J.-C. Poirier is with SIREHNA, Naval Group, 5 rue de l'Halbrane, 44340, Bouguenais, France (e-mail: jean-charles.poirier@sirehna.com).

S. Guillou is with the University of Caen, LUSAC, 60 rue Max-Pol Foucher, CS20082, Cherbourg, France (e-mail: sylvain.guillou@unicaen.fr).

Y. Méar is with CNAM-INTECHMER, Boulevard de Collignon, 50110, Tourlaville, France (e-mail: yann.mear@lecnam.net).

P. Mercier is with the University of Caen, LUSAC, 60 rue Max-Pol Foucher, CS20082, Cherbourg, France (e-mail: philippe.mercier@unicaen.fr).

E. Poizot is with CNAM-INTECHMER, Boulevard de Collignon, 50110, Tourlaville, France (e-mail: emmanuel.poizot@lecnam.net).

  

Fig. 1. Tidal turbine used for the experiment presented in Mycek *et al.* (2014) [4].

TABLE I
CHOSEN PARAMETERS FOR MODELLING THE TIDAL TURBINE [4]

| Quantity | Value | Unit |
|---|---|---|
| Flow speed $U_\infty$ | 0.8 | $m.s^{-1}$ |
| Turbine radius $R$ | 0.35 | $m$ |
| Tip Speed Ratio $TSR$ | 3.67 | ~ |
| Turbulent rate $I$ | $[3, 15]$ | % |

$$< U >= \sqrt{< U_x >^2 + < U_y >^2 + < U_z >^2}. \quad (3)$$

The Tip Speed Ratio is defined as: $TSR = \Omega_R R/U_\infty$, where $\Omega_R$ is the angular velocity of the rotor. The $TSR$ is chosen close to the operating point of the turbine. Force coefficients are calculated in Equation (4) and Equation (5):

$$C_T = \frac{F_x}{0.5\rho\Pi R^2 < U_{x_\infty} >^2}, \quad (4)$$

$$C_P = \frac{M_x\Omega_R}{0.5\rho\Pi R^2 < U_{x_\infty} >^3}, \quad (5)$$

where $F_x$ is the axial force acting on the whole turbine and $M_x$ is the axial torque acting on the rotor. Velocity in the wake is measured with a Laser Doppler Velocimetry (LDV) and the origin of the reference frame is the rotor center. Profiles in the wake are given in dimensionless unit: $U^* = U/U_\infty$ and $y^* = y/R$.

### B. Numerical models

*1) LBM approach:* The Lattice Boltzmann Method (LBM) is an unsteady CFD method. The study presented hereafter uses the Palabos open-source library. LBM predicts the fluid behaviour and comes from the Boltzmann equation. It describes the fluid from a mesoscopic point of view through distribution functions $f$. A distribution function represents a group of molecules at a given position and time which have a certain velocity. Evolution of distribution functions is governed by the Boltzmann equation given in Equation (6):

$$\frac{\partial f(\boldsymbol{x},\boldsymbol{\xi},t)}{\partial t} + \boldsymbol{\xi}.\nabla f(\boldsymbol{x},\boldsymbol{\xi},t) = \Omega(f(\boldsymbol{x},\boldsymbol{\xi},t), f(\boldsymbol{x},\boldsymbol{\xi},t)), \quad (6)$$

where $\Omega()$ is the collision operator representing collisions between molecules. It can take various forms. In the simulations presented afterwards, a recursive regularized collision operator is used. It is described in Malaspinas (2015) [7]. This operator is known in Palabos as the *completeRegularizedTRT* operator. TRT stands for two relaxation times.

The mesh used is Cartesian, as often in LBM simulations, and a constant space step $\Delta x$ is used. In LBM simulations, directions of propagation of molecules are constraint to a pre-defined set of directions of propagation. The sets available in Palabos are described in Qian *et al.* (1992) [8]. In this study, a set with 27 directions of propagation is used, it is usually denominated $D3Q27$. On each mesh node now lie 27 distribution functions $f_i$. LBM is solved into constant time steps, spaced by $\Delta t$. At each time step, two steps are required to solve the equation: a collision step and a streaming step. The collision step uses the collision operator to compute the new state of distribution functions. It is described in Equation (7):

$$f_i'(\boldsymbol{x},t) = \Omega(f_i(\boldsymbol{x},t)). \quad (7)$$

The streaming step is the propagation of post-collision distribution functions onto adjacent nodes according to the directions of propagation. It is described in Equation (8):

$$f_i(\boldsymbol{x} + \boldsymbol{c}_i\Delta t, t + \Delta t) = f_i'(\boldsymbol{x},t), \quad (8)$$

where $c_i$ are the directions of propagation of the chosen set.

In order to save computational resources, a static grid refinement is used. It is based on a multi-block approach and is described in Lagrava *et al.* (2012) [9]. Two adjacent levels have the following relations: $\Delta x_c = 2\Delta x_f$ and $\Delta t_c = 2\Delta t_f$, where $f$ refers to the fine level and $c$ to the coarse level.

The Large Eddy Simulation turbulence model is a Smagorinsky model. It is described in Malaspinas and Sagaut (2012) [10] and known in Palabos as the *consistent Smagorinsky* model. Since it is a constant Smagorinsky model, a damping of the Smagorinsky coefficient is set up close to the surface of the turbine. Far from the turbine, the value of the Smagorinsky constant is $C_s = 0.18$.

The turbine is modelled with an Immersed Boundary Method (IBM). The model used is described in Guo *et al.* (2002) [11]. A boundary layer model is included in the IBM algorithm to allow for a coarser mesh size around the turbine. The model modifies the velocity imposed by the IBM in order to match Spalding law of the wall [12].

*2) Navier-stokes approach:* Navier-Stokes LES simulations were carried out on Star-CCM+ software. The turbulence model is a SST k-$\omega$ DES. The convection scheme is a hybrid second order upwind/bounded central differencing scheme and the temporal scheme is second order accurate. A no-slip condition is used at the surface of the turbine.

### C. Upstream turbulence generation

Both LBM and NS approaches use Synthetic Eddy Methods (SEM), which were first introduced by Jarrin *et al.* (2009) [13]. The NS approach uses the original SEM of Jarrin while the LBM approach uses the Divergence Free SEM introduced by Poletto *et al.* (2013) [14]. The implementation and validation of a SEM in Palabos is presented in Grondeau *et al.* (2017) [15]. These methods allow for the generation of a turbulent flow that matches a specified Reynolds tensor. The tensor is chosen diagonal with all the diagonal terms equal. Diagonal terms are chosen in order to match with the measured turbulence rate: $3\ \%$ and $15\ \%$.

The size of the structures generated by the SEM, $L$, is chosen to $L = 1.0\ m$ for $I = 3\ \%$ and to $L = 1.2\ m$ for $I = 15\ \%$. This last value is twice larger than the one measured by Medina *et al.* (2017) [16]. This can induce some differences in the wake. Those values have been chosen after a dedicated study in order to maintain a high enough turbulence rate in the computational domain.

### D. Computational domains

The LBM computational domain is $14 \times 8 \times 8\ m$. The free-surface and the wall of the flume tank wall are not modelled for the sake of simplicity and because the blockage ratio is low ($0.048$). Thus, the turbine is placed in open water, far from the boundaries. Sides, top and bottom boundaries are velocity imposed boundary conditions. The outlet is a zero-gradient velocity boundary condition. The domain is divided into $5$ levels, each level has a different mesh size and time step. The rotor of the turbine is at the finest level where $\Delta x = 1.39 \times 10^{-3}\ m$, the stator is a level lower where $\Delta x = 2.78 \times 10^{-3}\ m$. Time step at the finest level is $7.8473 \times 10^{-5}\ s$. The maximum dimensionless mesh size at the finest level is $\Delta x^+ = 299$. The mesh has $82.68 \times 10^6$ elements, including $25 \times 10^6$ elements for the finest level. It takes $450\ h.CPU$ to compute one complete revolution of the rotor, where $h.CPU$ is the wall-clock-time multiplied by the number of $CPU$ used.

The NS computational domain is an unstructured mesh that fits the geometry. The domain is $14 \times 4 \times 2\ m$. The outlet is an imposed pressure condition and bottom and sides boundary conditions are no-slip conditions. The top boundary condition is a symmetry condition. The first mesh elements is $\Delta x^+ = 1$ away from the surface of the rotor, thus approximately $\Delta x = 3.0 \times 10^{-5}\ m$. The time step is $4.0 \times 10^{-3}\ s$. The mesh that envelops the rotor is a rotating mesh with overset grids. The total number of mesh elements is $20 \times 10^6$ elements. It takes $124\ h.CPU$ to compute a revolution.

A mesh convergence study has been carried out for both LBM-LES mesh and NS-LES mesh. Only force coefficients were considered during the convergence study. The LBM numerical domain is larger than the NS numerical domain. However, in the LBM numerical domain, the computational cost of extra meshes is insignificant compared to the cost of finest meshes. Fig. 2 shows the mesh sizes on the central line $y = z = 0\ m$ for LBM and NS mesh. The mesh size is constant in the $y$ and $z$ directions over a diameter large enough to account for wake expansion. LBM simulations were carried out after NS simulations and because LBM mesh sizes are constraint by the mesh size at the finest level, mesh sizes in the wake are slightly different.

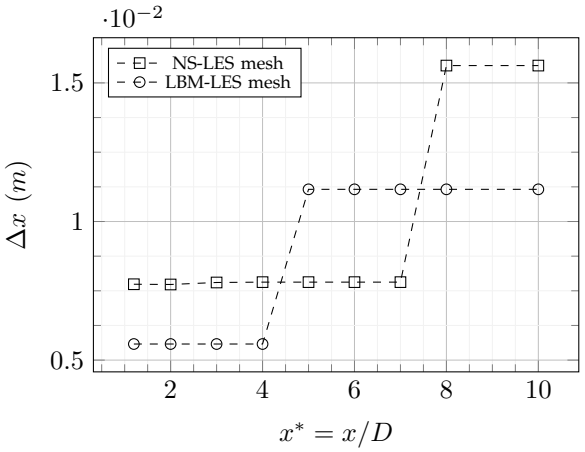


Fig. 2. Mesh size on the center line $y = z = 0\ m$ for LBM-LES and NS-LES simulations of tidal turbine [4].

## III. Results

In this section, the LBM and NS simulations are compared with the experiment described in Mycek *et al.* (2014) [4]. Force coefficients and average wake quantities are investigated for the case with $I = 3\ \%$ and $I = 15\ \%$. Forces and wake statistics are obtained after a convergence of $29.4$ revolutions for NS simulations and $21.3$ revolution for LBM simulations. Statistics are then calculated during $34.7$ revolutions for NS simulations and $16$ revolutions for LBM simulations.

### A. Case with I = 3 %

A snapshot of the instantaneous axial velocity calculated from the LBM simulation is given in Fig. 3. The wake is weakly influenced by the ambient turbulence.

Force coefficients are plotted in Table II. New quantities are introduced, the standard deviation of the thrust coefficient $\sigma_{C_T}$ and of the power coefficient $\sigma_{C_P}$.

Both approaches predicts the force coefficients quite well except for the standard deviation $\sigma_{C_P}$, which is strongly overestimated by the NS approach. NS results are closer to the experiment for other quantities. The boundary layer model used in the LBM simulation does not allow for an accurate computation of the flow close to the blades. It probably explains the differences. Nevertheless, LBM standard deviations are relatively close to experimental ones. Which is encouraging and shows that the model behave well with ambient turbulence.

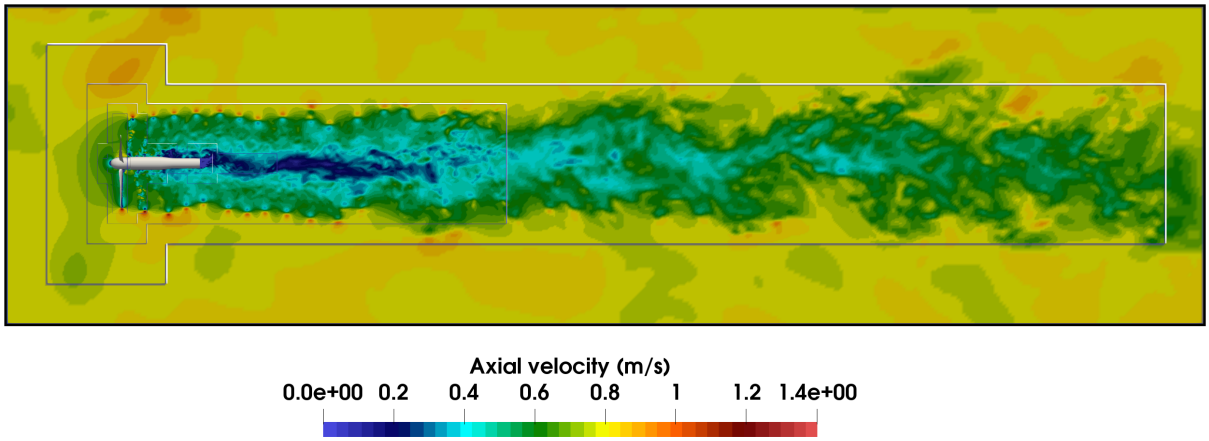


Fig. 3. Intanteneous axial velocity around the turbine of Mycek *et al.* (2014) [4]. LBM simulation at $TSR = 3.67$ with $I = 3$ %. Plane $xy$ at $z = 0$ $m$.

TABLE II
POWER COEFFICIENT $C_P$, THRUST COEFFICIENT $C_T$, STANDARD DEVIATION $\sigma_{C_T}$ AND $\sigma_{C_P}$ FROM MYCEK *et al.* (2014) [4] AND FROM LBM AND NS SIMULATIONS WITH $I = 3$ % AND $TSR = 3.67$.

| | $C_T$ | Difference | $C_P$ | Difference | $\sigma_{C_T}$ | Difference | $\sigma_{C_P}$ | Difference |
|---|---|---|---|---|---|---|---|---|
| Experiment | 0.805 | \ | 0.42 | \ | 0.034 | \ | 0.029 | \ |
| LBM-LES | 0.742 | −7.8 % | 0.50 | +19.7 % | 0.031 | −8.6 % | 0.035 | +14 % |
| NS-LES | 0.838 | +4.1 % | 0.49 | +16.8 % | 0.031 | −9.1 % | 0.060 | +109 % |

Average axial velocity profiles are plotted on Fig. 4. The velocity deficit in the close wake is well predicted by the NS approach. LBM profile at $x = 2$ $D$ is further away. The use of a boundary layer model and the coarser mesh close to the blades may cause those differences. In the medium and far wakes, the velocity deficit predicted by the LBM simulation is close to the experimental one. The velocity deficit is recover faster with the NS approach. By considering the mesh size in the wake for both approaches (Fig. 2), it could point out the fact that the LBM is less dissipative than the NS approach. However, there was no mesh convergence study for the NS approach.

Average turbulence intensity $I_{2D}$ profiles are given in Fig. 5. The turbulence intensity $I_{2D}$ is defined in Equation (9):

$$I_{2D} = 100\sqrt{\frac{0.5(< u_x^2 > + < u_y^2 >)}{< U_x >^2}}. \qquad (9)$$

As for the axial velocity, the NS approach gives better results in the close wake. Nevertheless, the turbulence peak at $y^* = \pm 0.5$ and $x = 2$ $D$ is well predicted by the LBM approach. This peak is most likely due to the tip-vortices generated by the blades. Both approaches seem well-suited for the turbulence prediction in the far wake.

To conclude, with a low ambient turbulence rate, both approaches provide relatively good results. The velocity deficit in the far wake is underestimated by the NS approach. A mesh sensibility study is needed to better understand this difference. Moreover, the turbine is modelled quite differently by the two approaches, which makes it even harder to conclude. Turbulence rate $I_{2D}$ and force coefficients $C_T$ and $C_P$ are well predicted by the two approaches.

### *B. Case with I = 15 %*

A snapshot of the instantaneous axial velocity calculated from the LBM simulation is given in Fig. 6. The wake is greatly affected by the ambient turbulence.

Force coefficients from the experiment and the NS and LBM simulations are summarized in Table III. LBM results are relatively close to the experiment and the differences are quite similar to those observed previously with $I = 3$ %. It may indicates that the model behave well with high turbulence intensity. Differences for the NS approach are larger. It is quite surprising since the NS approach does not use a wall modelling function and have a much finer mesh around the blades. It may be possible that the larger turbulent structures generated by the SEM increase force coefficients. A similar observation has been made by Blackmore *et al.* (2016) [3]. They noticed that the integral length scale of the turbulence can have a greater influence over force coefficients than the ambient turbulence rate.

Average axial velocity profiles from the experiment and NS and LBM simulations are plotted on Fig. 7. Both NS and LBM approaches show good agreement with experimental results. As it was observed on Fig. 6, the turbine footprint quickly disappears and is not visible at $x = 10$ $D$.

Turbulence intensity $I_{2D}$ profiles are plotted on Fig. 8. NS results match really well with experimental

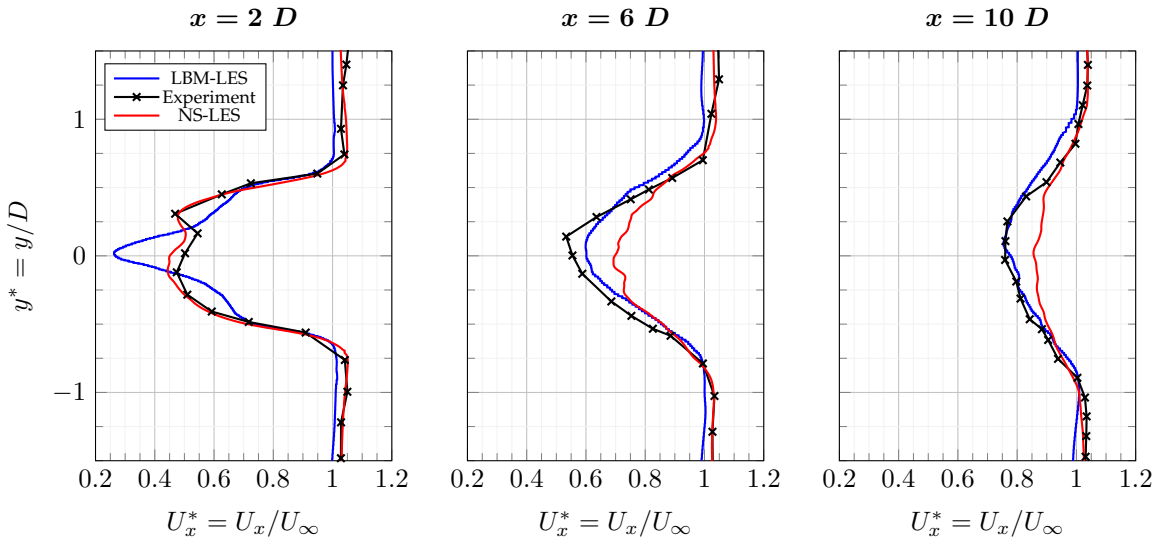


Fig. 4. Average axial velocity profiles in the wake of tidal turbine [4] at $TSR = 3.67$ and with $I = 3$ %.

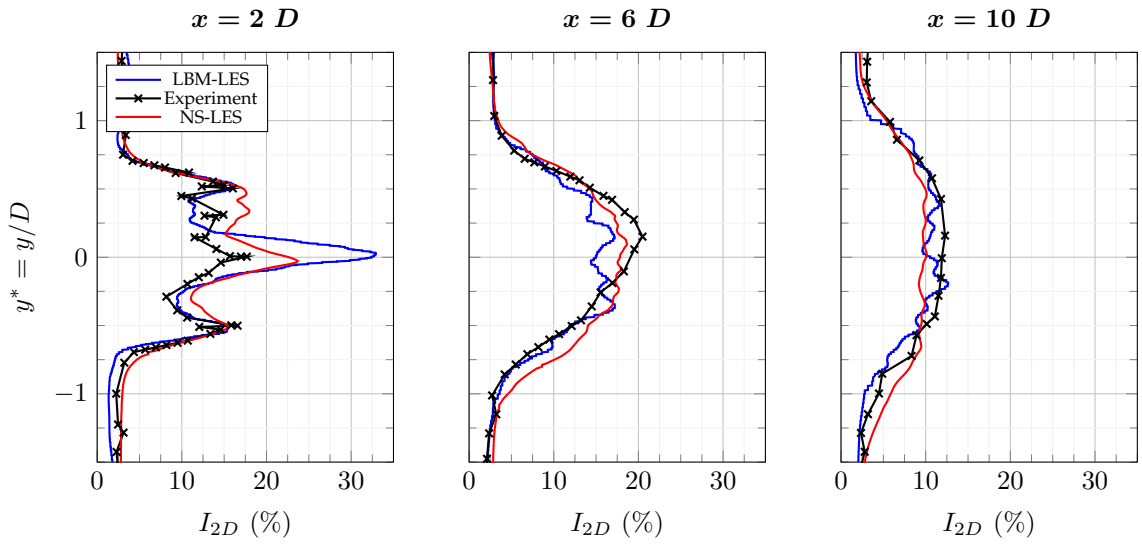


Fig. 5. Average tubulence intensity $I_{2D}$ profiles in the wake of tidal turbine [4] at $TSR = 3.67$ and with $I = 3$ %.

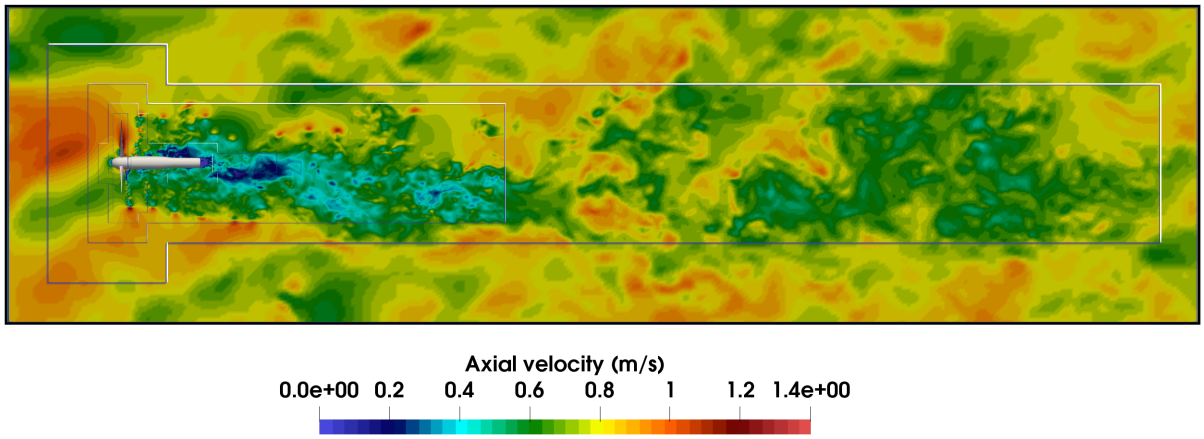


Fig. 6. Intanteneous axial velocity around the turbine of Mycek *et al.* (2014) [4]. LBM simulation at $TSR = 3.67$ with $I = 15$ %. Plane $xy$ at $z = 0\ m$.

ones. LBM under-predicts the turbulence intensity $I_{2D}$ in the close and far wake. It probably means that the turbine does not produce enough turbulence. The wall function may filter out stall phenomena that occur because of the high ambient turbulence, thus reducing the turbulence production. Numerical dissipation is probably not an issue here since the close wake was well predicted with $I = 3$ %.

TABLE III
POWER COEFFICIENT $C_P$, THRUST COEFFICIENT $C_T$, STANDARD DEVIATION $\sigma_{C_T}$ AND $\sigma_{C_P}$ FROM MYCEK *et al.* (2014) [4] AND FROM LBM AND NS SIMULATIONS WITH $I = 15$ % AND $TSR = 3.67$.

| | $C_T$ | Difference | $C_P$ | Difference | $\sigma_{C_T}$ | Difference | $\sigma_{C_P}$ | Difference |
|---|---|---|---|---|---|---|---|---|
| Experiment | 0.73 | \ | 0.374 | \ | 0.096 | \ | 0.084 | \ |
| LBM-LES | 0.70 | −4.4 % | 0.462 | +23.0 % | 0.101 | +5.2 % | 0.071 | −15 % |
| NS-LES | 0.85 | +16.0 % | 0.563 | +49.0 % | 0.14 | +45 % | 0.360 | +328 % |

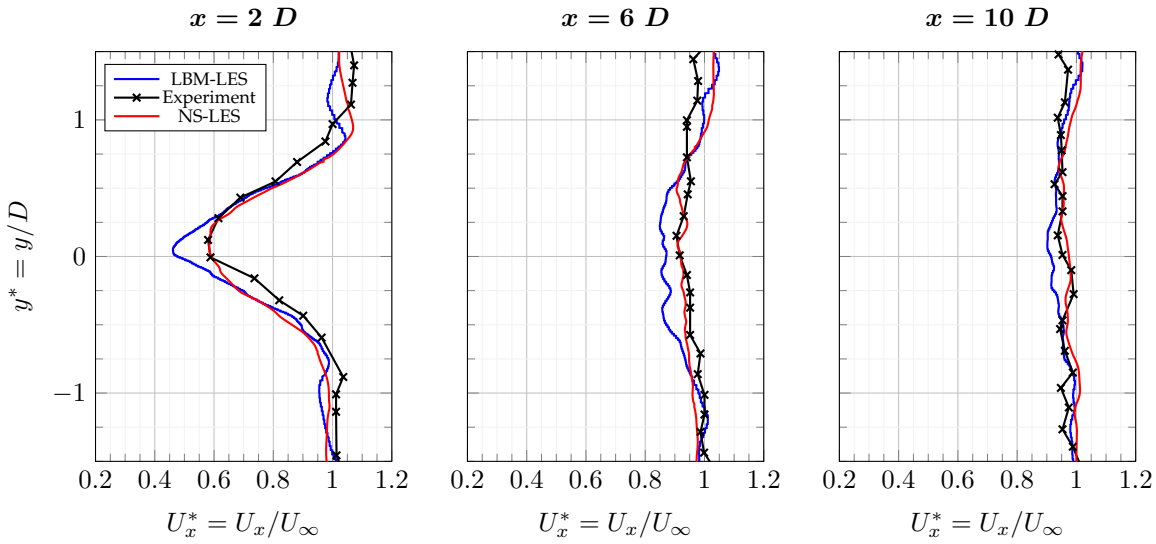


Fig. 7. Average axial velocity profiles in the wake of tidal turbine [4] at $TSR = 3.67$ and with $I = 15$ %.

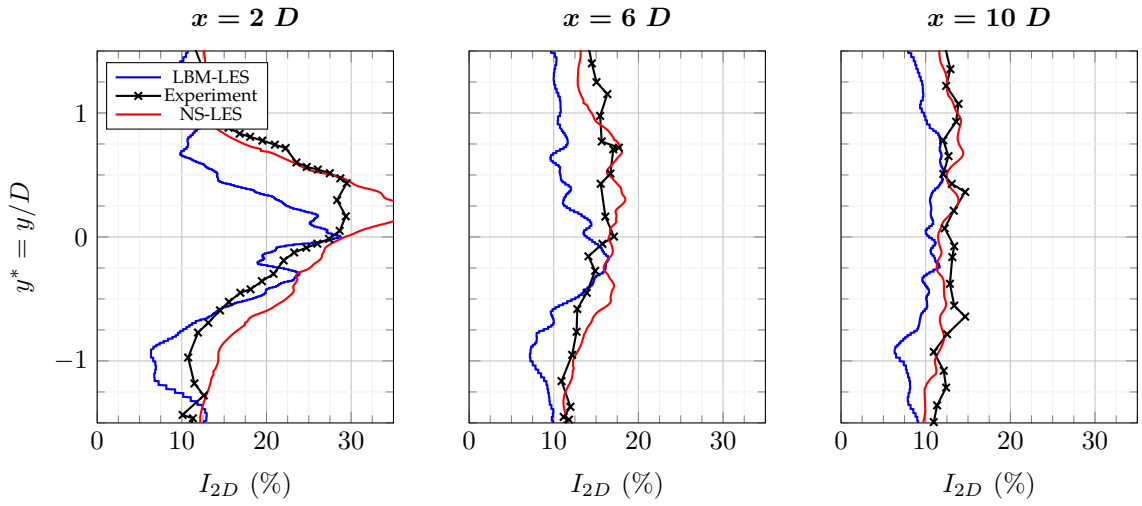


Fig. 8. Average tubulence intensity $I_{2D}$ profiles in the wake of tidal turbine [4] at $TSR = 3.67$ and with $I = 15$ %.

To conclude, LBM approach gives good predictions for force coefficients and wake average axial velocity. Turbulence intensity in the wake is slightly under-predicted. NS approach gives good wake prediction but high differences are observed for force coefficients.

## IV. CONCLUSION AND PROSPECTS

The simulation of a tidal turbine in a turbulent environment has been carried out with both LBM-LES approach and NS-LES approach. Both approaches are blade resolved and use synthetic eddy method for the turbulence generation. Simulations were compared to experimental results obtained from flume tank measurements.

It has been shown that both approaches provide relatively good wake predictions. With the LBM approach, differences are located in the close wake of the tidal turbine. The wall function is probably the source of it. Differences in the far wake have been observed for the NS approach. Considering that mesh sizes in the wake are close for both approaches, it is possible that the LBM is more appropriate for wake propagation.

The main disadvantages of the LBM approach is of course the Cartesian mesh, which forbids body fitted meshes and considerably increases the number of elements. As an example, even with a coarser mesh size around the blades, which requires a wall function,

the number of elements of the LBM mesh is 4 times larger than the NS mesh. The number of elements and computational time presented in section II do not reveal the true capacity of the LBM. Indeed, the IBM consumes a lot of computational resources and, because of its non-local approach, is not well adapted to the LBM.

To go further in characterizing the wake propagation capacity of both approaches, it would be interesting to compare the LBM approach with a relatively identical NS approach. Actuator methods would be appropriate since they do not need body fitted mesh nor IBM.

## ACKNOWLEDGEMENT

The authors would like to thank the SIREHNA company for supporting this work. The authors would also like to thank IFREMER for the data provided.

## REFERENCES

[1] E. Osalusi, J. Side, and R. Harris, "Structure of turbulent flow in emec's tidal energy test site," *International Communications in Heat and Mass Transfer*, vol. 30, pp. 422–431, 2009.

[2] T. Clark, "Turbulence in marine environments (time): A framework for understanding turbulence and its effects on tidal devices," in *EWTEC*, 2015.

[3] T. Blackmore, L. E. Myers, and A. S. Bahaj, "Effects of turbulence on tidal turbines: Implications to performance, blade loads, and condition monitoring," *International Journal of Marine Energy*, vol. 14, pp. 1–26, 2016.

[15] M. Grondeau, P. Mercier, S. Guillou, J. Poirier, E. Poizot, and Y. Mear, "Numerical simulation of a tidal turbine model in a turbulent flow with the lattice boltzmann method," in *Proceedings of the 12th European Wave and Tidal Energy Conference*, Cork, Ireland, 2017.

[4] P. Mycek, B. Gaurier, G. Germain, G. Pinon, and E. Rivaolen, "Experimental study of the turbulence intensity effects on marine current turbines behaviour. part i: One single turbine," *Renewable Energy*, vol. 66, pp. 729–746, 2014.

[5] P. Ouro and T. Stoesser, "Wake generated downstream of a vertical axis tidal turbine," in *Proceedings of the 12th European Wave and Tidal Energy Conference*, Cork, Ireland, 2017.

[6] U. Ahmed, D. D. Apsley, I. Afgan, T. Stallard, and P. K. Stansby, "Fluctuating loads on a tidal turbine due to velocity shear and turbulence: comparison of cfd with fields data," *Renewable Energy*, vol. 112, pp. 235–246, 2017.

[7] O. Malaspinas, "Increasing stability and accuracy of the lattice boltzmann scheme: recursivity and regularization," May 2015, arXiv:1505.06900v1 [physics.flu-dyn].

[8] Y. H. Qian, D. D'Humires, and P. Lallemand, "Lattice bgk models for the navier-stokes equations," *Europhysics Letters*, vol. 17, no. 6, pp. 479–484, 1992.

[9] S. Lagrava, W. Daniel, O. Malaspinas, J. Latt, and B. Chopard, "Advances in multi-domain lattice boltzmann grid refinement," *Journal of Computational Physics*, vol. 231, no. 14, pp. 4808–4822, 2012.

[10] O. Malaspinas and P. Sagaut, "Consistent subgrid scale modelling for lattice boltzmann methods," *Journal of Fluid Mechanics*, 2012.

[11] Z. Guo, C. Zheng, and B. Shi, "Discrete lattice effects on the forcing term in the lattice boltzmann method," *Physical Review*, 2002.

[12] D. Spalding, "A single formula for the law of the wall," *Journal of Applied Mechanics*, vol. 28, no. 3, pp. 455–458, 1961.

[13] N. Jarrin, R. Prosser, J.-C. Uribe, S. Benhamadouche, and D. Laurence, "Reconstruction of turbulent fluctuations for hybrid rans/les simulations using a synthetic-eddy-method," *International Journal of Heat and Fluid Flow*, vol. 30, pp. 435–442, 2009.

[14] R. Polleto, T. Craft, and A. Revell, "A new divergence free synthetic eddy method for the reproduction of inlet flow conditions for les," *Flow, Turbulence and Combustion*, vol. 91, no. 3, pp. 519–539, 2013.

[16] O. D. Medina, F. G. Schmitt, R. Calif, G. Germain, and B. Gaurier, "Turbulence analysis and multiscale correlations between synchronised flow velocity and marine turbine power production," *Renewable Energy*, vol. 112, pp. 314–327, 2017.